Central role of G protein Gαi2 and Gαi2$^+$ vomeronasal neurons in balancing territorial and infant-directed aggression of male mice

Anne-Charlotte Trouillet[a], Matthieu Keller[a], Jan Weiss[b], Trese Leinders-Zufall[b], Lutz Birnbaumer[c,d,1], Frank Zufall[b,1], and Pablo Chamero[a,1]

[a]Laboratoire de Physiologie de la Reproduction et des Comportements, UMR Institut National de la Recherche Agronomique (INRA)-CNRS-Institut Français du Cheval et de l'Equitation (IFCE)-University of Tours, 37380 Nouzilly, France; [b]Center for Integrative Physiology and Molecular Medicine, Saarland University, 66421 Homburg, Germany; [c]Neurobiology Laboratory, National Institute of Environmental Health Sciences, National Institutes of Health, Durham, NC 27709; and [d]Institute of Biomedical Research (BIOMED), School of Medical Sciences, Catholic University of Argentina, C1107AAZ Buenos Aires, Argentina

Contributed by Lutz Birnbaumer, January 23, 2019 (sent for review December 18, 2018; reviewed by Peter A. Brennan and Marc Spehr)

Aggression is controlled by the olfactory system in many animal species. In male mice, territorial and infant-directed aggression are tightly regulated by the vomeronasal organ (VNO), but how diverse subsets of sensory neurons convey pheromonal information to limbic centers is not yet known. Here, we employ genetic strategies to show that mouse vomeronasal sensory neurons expressing the G protein subunit Gαi2 regulate male–male and infant-directed aggression through distinct circuit mechanisms. Conditional ablation of Gαi2 enhances male–male aggression and increases neural activity in the medial amygdala (MeA), bed nucleus of the stria terminalis, and lateral septum. By contrast, conditional Gαi2 ablation causes reduced infant-directed aggression and decreased activity in MeA neurons during male–infant interactions. Strikingly, these mice also display enhanced parental behavior and elevated neural activity in the medial preoptic area, whereas sexual behavior remains normal. These results identify Gαi2 as the primary G protein α-subunit mediating the detection of volatile chemosignals in the apical layer of the VNO, and they show that Gαi2$^+$ VSNs and the brain circuits activated by these neurons play a central role in orchestrating and balancing territorial and infant-directed aggression of male mice through bidirectional activation and inhibition of different targets in the limbic system.

olfactory | GCamp6f | V1R receptor | infant-directed aggression | territorial aggression

Aggression is an innate social behavior most commonly displayed in males, typically directed to other males of the same species (1) or to another male's offspring (2). Such behaviors are important for resource competition, establishment of group hierarchies, and access to sexual partners. For example, pup-directed aggression resulting in infanticide ultimately induces endocrine changes in females, which makes them quickly receptive to a male newcomer (3) and thus increases reproductive success. In rodents, the role of the olfactory system is critical for initiating aggression. Pheromonal cues present in secretions from adult males or pups are detected by distinct subsets of sensory neurons in the vomeronasal organ (VNO) (4–7) to initiate neural signals that, in turn, trigger aggressive behavior. However, many of the cellular and molecular mechanisms underlying such aggression-promoting signaling remain unknown.

The mouse VNO contains two major populations of vomeronasal sensory neurons (VSNs): VSNs of the apical layer of the vomeronasal sensory epithelium (VNE) express the G protein Gαi2 and members of the V1R family of vomeronasal G protein-coupled receptors, whereas VSNs of the basal layer express Gαo and members of the V2R receptor family (8–14). Gαo-expressing (i.e., Gαo$^+$) cells have been implicated in male–male aggression by detecting urine-derived high molecular weight (HMW) pheromones, particularly MUP proteins, and ESP1 peptide, both of which are capable to induce aggression (15–19). Conditional ablation of Gαo eliminates VSN transduction of MUPs and ESP1 as well as male–male aggression (16, 20, 21). However, organic low molecular weight (LMW) molecules recognized by Gαi2 VSNs can also induce aggression (22). Furthermore, mice carrying a global deletion of Gαi2 are less aggressive (23), suggesting that both VSN populations may interact to generate aggressive behavior. Thus, whether each VNO subsystem activates independent aggression circuits or whether the two subsystems function in a cooperative and integrative manner to generate territorial aggression is not yet clear.

Infanticidal behavior, in which an adult attacks and kills an alien pup, is observed in virgin adult males and is highly dependent on the VNO. Genetic deletion of the transient receptor potential channel Trpc2, the primary sensory ion channel of VSNs, or surgical VNO ablation strongly reduce aggression toward pups (24, 25). Pup odors in virgin males preferentially activate a region of the accessory olfactory bulb (OB; AOB) innervated by Gαi2 neurons (25), but how molecularly defined VSN subsets influence pup-directed aggression remains unclear. Several regions in the limbic brain are activated during infanticide and male–male aggression, including the medial amygdala (MeA), the bed nucleus of the stria terminalis (BNST),

Significance

Male mice detect pheromones that trigger aggressive behavior toward other males or another male's pups. We found that a subpopulation of chemosensory neurons in the vomeronasal organ organizes and balances both types of aggression by reducing or enhancing each behavioral output. These neurons use a signaling cascade that requires the G protein Gαi2 in the detection of volatile pheromones and steroid derivatives. This subset of sensory neurons conveys pheromonal information to limbic centers in the brain through independent mechanisms, targeting different groups of neurons during male–male or infant-directed aggression. How the mouse olfactory system detects and processes pheromones that trigger different forms of aggression should aid in the identification of neural networks mediating male–male vs. infant-directed social aggression.

Author contributions: M.K., T.L.-Z., L.B., F.Z., and P.C. designed research; A.-C.T., J.W., T.L.-Z., and P.C. performed research; L.B. contributed new reagents/analytic tools; A.-C.T., J.W., T.L.-Z., and P.C. analyzed data; and A.-C.T., F.Z., and P.C. wrote the paper.

Reviewers: P.A.B., University of Bristol; and M.S., RWTH Aachen University.

The authors declare no conflict of interest.

Data deposition: The datasets generated and/or analyzed during the present study are available in the Data Inra Dataverse portal (https://data.inra.fr/).

[1]To whom correspondence may be addressed. Email: Birnbau1@gmail.com, frank.zufall@uks.eu, or pablo.chamero-benito@inra.fr.

This article contains supporting information online at www.pnas.org/lookup/suppl/doi:10.1073/pnas.1821492116/-/DCSupplemental.

and the ventromedial hypothalamus (VMH) (25, 26). Current understanding of these neuronal substrates is insufficient to explain whether infanticide and male–male aggression are initiated by the same or different subsets of VSNs. Furthermore, it is not known whether the same or different groups of neurons from these common limbic structures are activated during male–male or infant-directed aggression. One possibility is that neuronal circuits originating from Gαi2^{+} VSNs may independently coordinate infant-directed and male–male aggression.

Because the *Gnai2* gene, which encodes Gαi2, is ubiquitously expressed in the developing brain and cortex (27, 28), analysis of VNO-dependent behaviors in mice carrying a global Gαi2 deletion (28) is impeded. Furthermore, no functional recordings in single VSNs lacking Gαi2 have been performed. To overcome these limitations, we have generated mice harboring a conditional deletion of Gαi2 in the olfactory system. These mice show a striking reduction in the sensory response to LMW organic molecules, demonstrating that Gαi2 is an obligate requirement for normal signaling of apical VSNs. Furthermore, territorial aggression is enhanced in these mutant mice, whereas infant-directed aggression is strongly diminished. Together with c-Fos mapping in aggression-controlling brain centers, our study establishes a critical role of Gαi2, the VSNs that express this G protein, and the circuits derived from Gαi2^{+} VSNs in orchestrating and balancing territorial and infant-directed aggression of male mice.

Results

Conditional Deletion of Gαi2 in VSNs. We used the Cre-*loxP* system to create mice with a tissue-specific and time-dependent deletion of Gαi2. Mice carrying a floxed allele of *Gnai2* (*Gnai2*$^{fx/fx}$) (29) were crossed with OMP-Cre mice (30, 31), in which the coding region for olfactory marker protein (OMP) is replaced by that of Cre recombinase. Conditional Gαi2 mutants (cGαi2$^{-/-}$) were heterozygous for *Cre* (*Gnai2*$^{fx/fx}$*Omp*$^{cre/+}$); mice heterozygous for both alleles (*Gnai2*$^{fx/+}$*Omp*$^{cre/+}$) served as controls (cGαi2$^{+/-}$). All experiments were performed with adult male mice (8–12 wk old).

We used immunohistochemistry (IHC) to examine the VNE in cGαi2$^{+/-}$ and cGαi2$^{-/-}$ males. Gαi2 immunoreactivity was absent in the VNE of cGαi2$^{-/-}$ mice, confirming the loss of Gαi2 protein expression (Fig. 1*A*). Staining was positive for markers of basal (V2R2, family C V2Rs), apical (PDE4A, phosphodiesterase 4A), or both (OMP) VSN populations in control and mutant mice (Fig. 1*A* and *SI Appendix*, Fig. S1*A*), showing that general tissue structure remained intact. By using RT-PCR with whole VNO cDNA from cGαi2$^{+/-}$ or cGαi2$^{-/-}$ males, we identified transcripts for several *V1r* receptors and two *V2r* receptors, *Trpc2* and *Plcb2*, in both genotypes (*SI Appendix*, Fig. S1*B*), indicating that expression of transduction molecules also remained intact. Quantitative RT-PCR analyses showed that relative expression of *Gnai2* in the VNO of cGαi2$^{-/-}$ males was reduced by 1.86 fold ($P < 0.001$), whereas *Gnao* expression increased by 1.47 fold ($P < 0.01$; Fig. 1*B*). *Gnai2* expression in the main olfactory epithelium (MOE) of control vs. mutant mice was not significantly different (Fig. 1*B*).

Previous work indicated a role for G protein α-subunits in the survival of VSNs (16, 23, 32). We analyzed PDE4A immunoreactivity, specific for the apical Gαi2-expressing zone (33), and the volume of apical and basal VNE layers in cGαi2$^{+/-}$ and cGαi2$^{-/-}$ mice. The volume of the apical layer was reduced by 1.41 fold whereas that of the basal layer increased 1.35-fold in cGαi2$^{-/-}$ mice ($P < 0.001$; Fig. 1*C*). Cell density remained unchanged (*SI Appendix*, Fig. S1*C*), indicating that the volume reduction of the apical layer likely resulted from a decrease in the number of VSNs. A reduced volume was also detected in whole AOB of cGαi2$^{-/-}$ mice as shown by IHC for OMP (13% reduction; $P < 0.001$; *SI Appendix*, Fig. S1*D*). By using IHC for Gαo, we found a reduced glomerular layer in the rostral AOB (31% reduction; $P < 0.001$), the primary target of Gαi2^{+} VSNs (*SI Appendix*, Fig. S1*D*). The general structure of MOE and glomerular layer of the main OB (MOB) remained unchanged in cGαi2$^{-/-}$ mice (*SI Appendix*, Fig. S1*E*). Thus, conditional Gαi2 deletion caused a selective loss of apical PDE4A-expressing VSNs and rostral AOB glomerular volume. We confirmed that general olfactory performance remained normal in cGαi2$^{-/-}$ males by performing several behavioral tests. There was no significant difference between cGαi2$^{-/-}$ and cGαi2$^{+/-}$ males in a food-finding test (*SI Appendix*, Fig. S1*F*). Likewise, novel odor investigation of female urine and odor discrimination of normal male urine vs. castrated male urine using a habituation–dishabituation paradigm (20, 31) revealed no significant differences between the two genotypes (*SI Appendix*, Fig. S1*G*). Thus, cGαi2$^{-/-}$ mice do not display any obvious defects with respect to main olfactory system function.

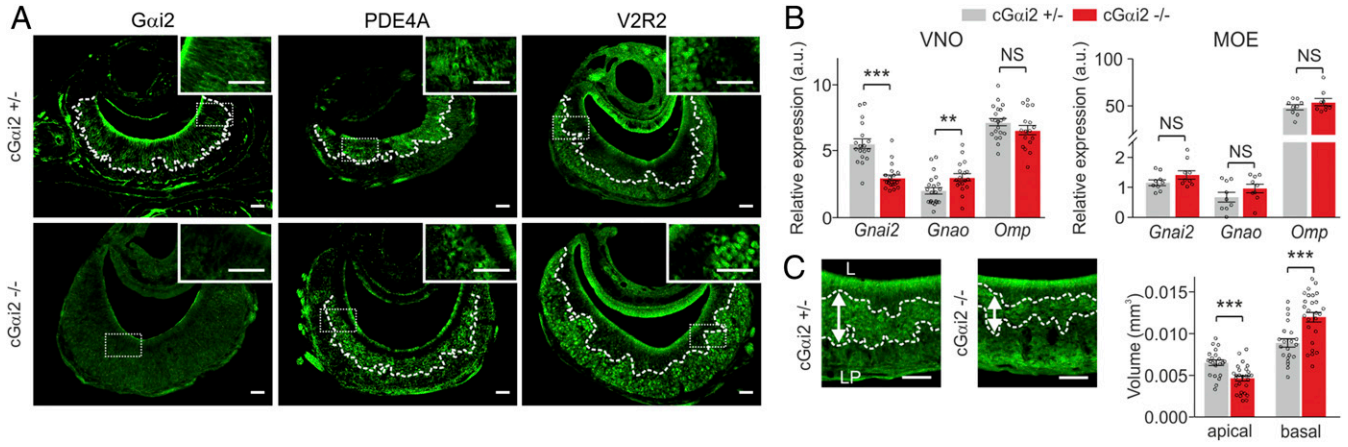

Fig. 1. Expression of marker proteins in the VNO of cGαi2$^{+/-}$ and cGαi2$^{-/-}$ mice. (*A*) Loss of Gαi2 immunoreactivity in cGαi2$^{-/-}$ VNO. Antibodies specific for PDE4A (apical layer) or V2R2 (basal layer) indicate that the laminar VNO organization persists in the absence of Gαi2. (Scale bars, 50 μm.) (*B*) Relative expression (normalized to *Hprt-1*) of *Gnai2*, *Gnao*, and *Omp* genes in VNO (*Left*) and MOE (*Right*). *Gnai2* expression decreased and *Gnao* expression increased, whereas *Omp* expression did not change, in cGαi2$^{-/-}$ VNO [$^{**}P < 0.01$ and $^{***}P < 0.001$; nonsignificant (NS), $P = 0.21$, Mann–Whitney *U* test; cGαi2$^{+/-}$, $n = 20$; cGαi2$^{-/-}$, $n = 18$]. No difference in gene expression in the MOE between the two genotypes was observed (NS, $P = 0.22$–0.53, Mann–Whitney *U* test). (*C*) Analysis of apical and basal VNO layer volume distinguished by PDE4A immunostaining indicates a significant reduction in the apical VNO layer [*t* test, $t(46) = 3.975$; $^{***}P < 0.001$] and an increase in basal VNO layer [*t* test, $t(46) = 3.929$; $^{***}P < 0.001$] of cGαi2$^{-/-}$ ($n = 27$) vs. cGαi2$^{+/-}$ mice ($n = 21$). L, lumen; LP, lamina propria. Data are expressed as means ± SEM. (Scale bars, 50 μm.)

Gαi2 Is Required for Sensory Function of Apical VSNs. VSNs that detect small organic pheromones and steroid derivatives localize to the apical VNO and express V1Rs and Gαi2 (34–37). These neurons do not recognize peptides or proteins (16). To determine whether Gαi2 is required for sensory signaling in apical VSNs, we performed live-cell Ca^{2+} imaging by using dissociated cells (15, 16, 21) and acute VNO slices (33, 34, 38) in combination with the Ca^{2+} sensors GCaMP6f, fura-2/AM, or fluo-4/AM (Fig. 2 and *SI Appendix*, Fig. S2). We crossed *Gnai2*$^{fx/fx}$ *Omp*$^{cre/cre}$ and *Rosa26*-floxstop-GCaMP6f mice (*Methods*) to drive expression of GCaMP6f in *Omp*$^{+}$, *Gnai2*-deficient cells. As chemostimuli, we used nine single compounds (four small organic molecules and five sulfated steroids) or a mix of five sulfated steroids (*SI Appendix*, Fig. S2*A*). Subsets of VSNs from heterozygous controls responded reliably to each of these stimuli (Fig. 2 and *SI Appendix*, Fig. S2 *C–F*). By contrast, such responses were severely diminished or absent in cGαi2$^{-/-}$ VSNs (Fig. 2 and *SI Appendix*, Fig. S2 *C–F*). The response rates of cGαi2$^{-/-}$ VSNs for these ligands were close to those of *Trpc2*$^{-/-}$ VSNs (Fig. 2*B*), indicating a nearly complete loss of sensory function in the apical layer. Importantly, Ca^{2+} responses to a mix of four MHC-binding peptides, known to activate V2R/Gαo^{+} VSNs (19, 33, 38, 39), and high-K^{+} solution remained intact (Fig. 2). Responses to MHC peptides also remained unaffected in *Trpc2*$^{-/-}$ VSNs, consistent with previous results (40). Together, these data establish that Gαi2 is

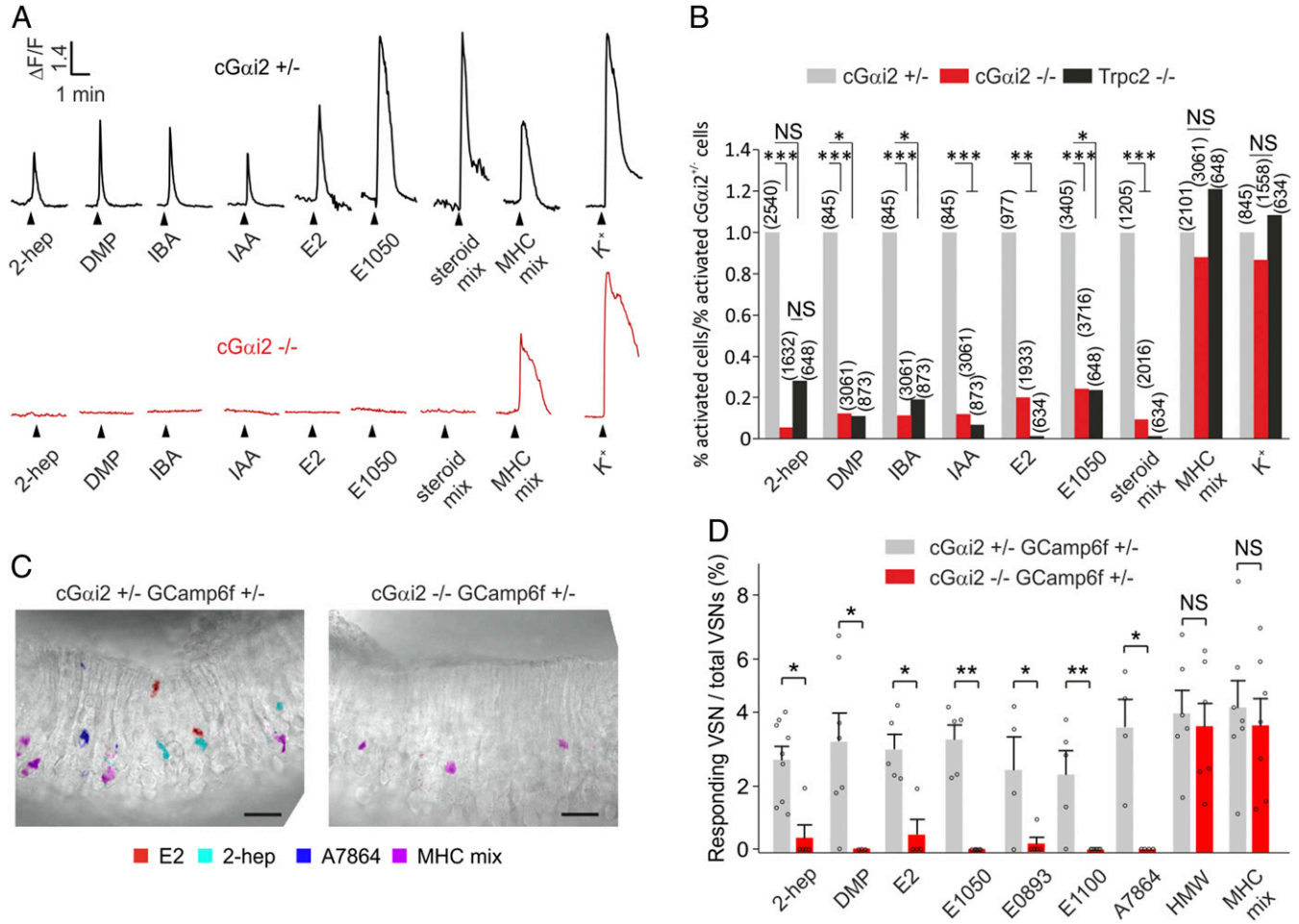

Fig. 2. Essential role of Gαi2 in molecular sensing by apical VSNs. (*A*) Representative Ca^{2+} responses imaged in dissociated VSNs from cGαi2$^{+/-}$ and cGαi2$^{-/-}$ mice. Cells were stimulated with the following stimuli known to activate V1R/Gαi2- or V2R/Gαo-expressing VSNs: 2-heptanone (2-hep, 10^{-8} M); dimethylpyrazine (DMP, 10^{-6} M); isobutylamine (IBA, 10^{-7} M); isoamylamine (IAA, 10^{-7} M); β-estradiol (E2, 1 μM); 1,3,5(10)-estratrien-3,17β-diol disulfate (E1050, 1 μM); sulfated steroid mix E1050, E1100 [1,3,5(10)-estratrien-3,17β-diol 3-sulfate], E0893 [1,3,5(10)-estratrien-3,17α-diol 3-sulfate], and A7864 (5-androsten-3β,17β-diol disulfate), 1 μM each; MHC peptide mix (MHC mix; SYFPEITHI, SYIPSAEKI, AAPDNRETF, SIINFEKL, 10^{-10} M each), and high (50 mM) KCl solution (K^{+}) as viability control. Note that cells from Gαi2$^{-/-}$ mice did not produce Ca^{2+} responses to the V1R ligands but did produce responses to the Gαo-dependent MHC peptide mix and high K^{+}. (*B*) Analysis of ligand-evoked Ca^{2+} responses in dissociated cells from cGαi2$^{+/-}$, cGαi2$^{-/-}$, and Trpc2$^{-/-}$ mice. Data are expressed as the percentage of responding cells to a given stimulus divided by the percentage of responding cells in the cGαi2$^{+/-}$ controls [*$P < 0.05$, **$P < 0.01$, ***$P < 0.001$; nonsignificant (NS), $P = 0.07$–0.63, Fisher's exact test]. Number of cells analyzed is indicated above each bar. Each stimulus was tested in 3–16 mice. (*C*) Spatial activation patterns obtained through GCaMP6f imaging in cGαi2$^{+/-}$ and cGαi2$^{-/-}$ VNO slices. Slices were stimulated with the steroids E2 (1 μM; red) and A7864 (1 μM; blue), 2-hep (10^{-8} M; cyan), and MHC mix (SYFPEITHI, SYIPSAEKI, AAPDNRETF, SIINFEKL, 10^{-10} M each; magenta). Stimulus-induced ΔF peak images were digitally superimposed onto the transmitted light image of the same slice (*Methods*; original ΔF peak images are shown in *SI Appendix*, Fig. S2). VSNs in cGαi2$^{-/-}$ slices responded to the MHC peptide mix but not to agonists of apical VSNs. (Scale bar, 25 μm.) (*D*) Percentage of responding VSNs/total VSNs in Gαi2$^{-/-}$ slices is strongly diminished or reduced to zero with stimuli known to activate apical VSNs ($\chi^2 = 40.8$, $P < 0.001$, Kruskal–Wallis ANOVA; *$P < 0.05$, **$P < 0.01$, Mann–Whitney *U* test; $n = 2$–3 slices per mouse from 7 cGαi2$^{+/-}$ and 5 cGαi2$^{-/-}$ GCaMP6f mice). No significant difference in the detection of Gαo-dependent stimuli is observed between the two genotypes [HMW, $t(10) = 0.36$; NS, $P = 0.72$; MHC mix, $t(12) = 0.44$; NS, $P = 0.66$]. Dots indicate the percentage of responding/total VSNs in independent slice recordings. Stimuli were tested one to three times per slice. Each stimulus was tested in at least three mice. Data are expressed as means ± SEM.

required for VSN sensory transduction in the apical VNE layer and plays a central role in detecting small organic molecules and steroid derivatives.

Normal Male Sexual Behavior in Gαi2 Mutants. Trpc2$^{-/-}$ male mice exhibit pronounced alterations in sexual behavior, including elevated mounting and courtship behaviors toward other males (41, 42). To determine whether Gαi2 is also required for male sexual behavior, we first measured serum testosterone levels and the weight of sexual organs (testes, preputial glands, seminal vesicles), but found no significant differences between cGαi2$^{-/-}$ and cGαi2$^{+/-}$ males (*SI Appendix*, Fig. S3 *A* and *B*). We next analyzed sexual behaviors toward females in sexually naïve cGαi2$^{-/-}$ and cGαi2$^{+/-}$ males (*SI Appendix*, Fig. S3 *D–G*). cGαi2$^{-/-}$ and cGαi2$^{+/-}$ males displayed the same level of preference for estrous female urine volatiles and nonvolatiles (*SI Appendix*, Fig. S3*C*). We also scored the number of animals mounting an intruder (female, male, or castrated male) and the mounting episodes (*SI Appendix*, Fig. S3*D*). cGαi2$^{-/-}$ and cGαi2$^{+/-}$ males showed robust mounting and a short latency to mount females, but very rarely displayed sexual behavior toward male or castrated male intruders. Next, we scored the latency to mount female intruders and to ejaculate, and the total mating time (*SI Appendix*, Fig. S3 *E* and *F*). Latency to ejaculate and total mating time of cGαi2$^{-/-}$ males were statistically indistinguishable from those of cGαi2$^{+/-}$ males (P = 0.21–0.89). We further assessed male courtship behavior by measuring ultrasonic vocalizations at high frequencies (30–110 kHz) emitted by resident males. cGαi2$^{-/-}$ and cGαi2$^{+/-}$ males produced high numbers of vocalizations in response to female intruders, whereas few vocalizations were produced during male–male investigation, and there was no significant difference between genotypes (*SI Appendix*, Fig. S3*G*). Together, these findings reveal that cGαi2$^{-/-}$ males display normal sexual behaviors and sexual motivation.

Territorial Aggression Is Enhanced in Gαi2 Mutant Males. Conditional deletion of Gαo in VSNs eliminated male–male aggression (16). This effect could result from cooperation of Gαo and Gαi2 subsystems, or the Gαi2 subsystem could operate relatively independently, being dispensable for aggression and/or controlling a parallel aggression circuit. To distinguish between these hypotheses, we compared territorial aggression of adult cGαi2$^{-/-}$ male mice vs. age-matched cGαi2$^{+/-}$ males in the resident–intruder paradigm (15, 16) (Fig. 3*A*).

Surprisingly, the number of animals attacking an adult male intruder was significantly higher in cGαi2$^{-/-}$ (25 of 27 mice; 93%) vs. cGαi2$^{+/-}$ residents (15 of 23 mice; 65%; $P < 0.05$; Fig. 3*A*), but there was no difference in the intruder investigation time for each genotype (*SI Appendix*, Fig. S4*A*). Total attack duration in three consecutive 10-min trials was high in cGαi2$^{-/-}$ and cGαi2$^{+/-}$ males (130 and 78 s, respectively; $P < 0.05$), showing that Gαi2 is dispensable for the display of aggression. By contrast, castrated male intruders consistently induced less aggression in control cGαi2$^{+/-}$ male residents (37 s; 50% reduction; $P < 0.05$; Fig. 3*A*), whereas attack duration to castrated males was approximately threefold higher in cGαi2$^{-/-}$ residents (129 s; $P < 0.01$) and did not differ from the level of aggression to intact male intruders ($P = 0.8$). Thus, there was no loss of territorial aggression in cGαi2$^{-/-}$ male residents.

Previous work has shown that the HMW (>10 kDa) and LMW (< 10 kDa; includes small peptides) fractions of urine from adult male mice can induce aggression in male residents (15, 16). Therefore, we tested whether cGαi2$^{-/-}$ VSNs are capable of detecting these two fractions. We used Ca^{2+} imaging in cGαi2$^{-/-}$, cGαi2$^{+/-}$, and Trpc2$^{-/-}$ VSNs to record responses to whole urine and the HMW and LMW fractions (Fig. 3*B*). All fractions induced large responses in cGαi2$^{+/-}$ VSNs: 592 of 4,698 cells screened (12%) responded to urine, 250 of 4,698 to LMW fractions (5%), and 402 of 5,577 (7%) to HMW fractions. In cGαi2$^{-/-}$, urine responses were reduced by half (215 of 3,366 activated cells; 6%; $P < 0.001$) and LMW fraction responses by approximately 60% (74 of 3,366; 2%; $P < 0.001$), whereas HMW responses were identical or even slightly elevated (551 of 5,797; 9%; $P = 0.2$; Fig. 3*B*). We identified activated cells by combining Ca^{2+} imaging with post hoc immunostaining (*SI Appendix*, Fig. S2*B*) (15, 16) using antibodies against PDE4A and Gαo (Fig. 3*C*). The vast majority of cells activated by HMW were Gαo^{+} in cGαi2$^{-/-}$ and control VSNs. LMW fraction and castrated male urine activated Gαo^{+} and PDE4A^{+} control VSNs, but nearly all cGαi2$^{-/-}$ activated cells were negative for PDE4A (Fig. 3*C* and *SI Appendix*, Fig. S4*B*). Together, these results indicate that activation of the Gαo^{+} VSN subpopulation is sufficient to induce intermale aggression, irrespective of whether this aggression is promoted by HMW or LMW urine fractions or castrated male urine.

Increased Brain Activation to Male Intruder in Gαi2 Mutant Males. To strengthen these results, we mapped in vivo brain activation in nine distinct regions of the central nervous system implicated in aggression (26) by using immunodetection of the immediate early gene c-Fos. These analyses included subdivisions of the MeA [posterodorsal MeA (MeApd) and posteroventral MeA (MeApv) divisions] and VMH [dorsomedial VMH (VMHdm) and ventrolateral VMH (VMHvl)], the posteromedial part of the medial division of the BNST (BNSTmpm), medial preoptic area (MPOA), and lateral septum (LS). Nonstimulated cGαi2$^{-/-}$ and cGαi2$^{+/-}$ males showed equivalent levels of basal c-Fos activity in all nine brain regions (*SI Appendix*, Fig. S4*C*). Exposure to adult male intruders induced a significant increase in the number of c-Fos^{+} nuclei in three of these regions: MeApd, BNSTmpm, and LS (Fig. 3 *D* and *E*). We did not observe significant differences in some other regions implicated in aggression, such as the VMH (Fig. 3*E*).

Male–male aggression and male pheromones activate a specific subpopulation of MeA neurons that are GABAergic and positive for the androgen receptor (AR) (43, 44). We used double-label IHC for c-Fos and AR, GABA, calbindin (CB), or calretinin (CR) to identify the MeA neurons activated in our experiments. In cGαi2$^{-/-}$ and cGαi2$^{+/-}$ males, c-Fos^{+} nuclei largely colocalized with AR (Fig. 3 *F* and *G*) and GABA, but not with CB and CR (*SI Appendix*, Fig. S4*D*). Moreover, the proportion of c-Fos^{+} neurons positive for AR was even larger in cGαi2$^{-/-}$ males, whereas no change was observed in the absolute number of AR^{+} neurons (Fig. 3*G*). Therefore, conditional Gαi2 deletion resulted in increased neural activation of a population of GABAergic, AR^{+} neurons in the MeA following exposure to a male intruder.

Infant-Directed Aggression Is Diminished in Gαi2 Mutant Males, but Parental Behavior Is Enhanced. Infanticidal behavior in mice, in which an adult attacks and kills a pup, is observed in virgin adult male mice and depends strongly on a functional VNO (24, 25). We investigated infant-directed behavioral consequences of the Gαi2 deletion. We exposed virgin males to 1–2-d-old pups and found that the number of aggressive animals was drastically reduced, whereas attack latency was significantly increased in cGαi2$^{-/-}$ males vs. heterozygous controls ($P < 0.01$; Fig. 4 *A* and *B*). Moreover, two critical measures of parenting behavior—pup grooming and pup retrieval—were significantly increased in cGαi2$^{-/-}$ males ($P < 0.05$ and $P < 0.01$; Fig. 4*B*). Thus, the display of pup-directed aggression is strongly decreased, whereas parental behavior is enhanced, in Gαi2 mutant males.

We used Fos immunodetection to examine whether the lack of apical/Gαi2^{+} sensory inputs alters neural activity in aggression-controlling brain centers during infant-directed aggression (Fig.

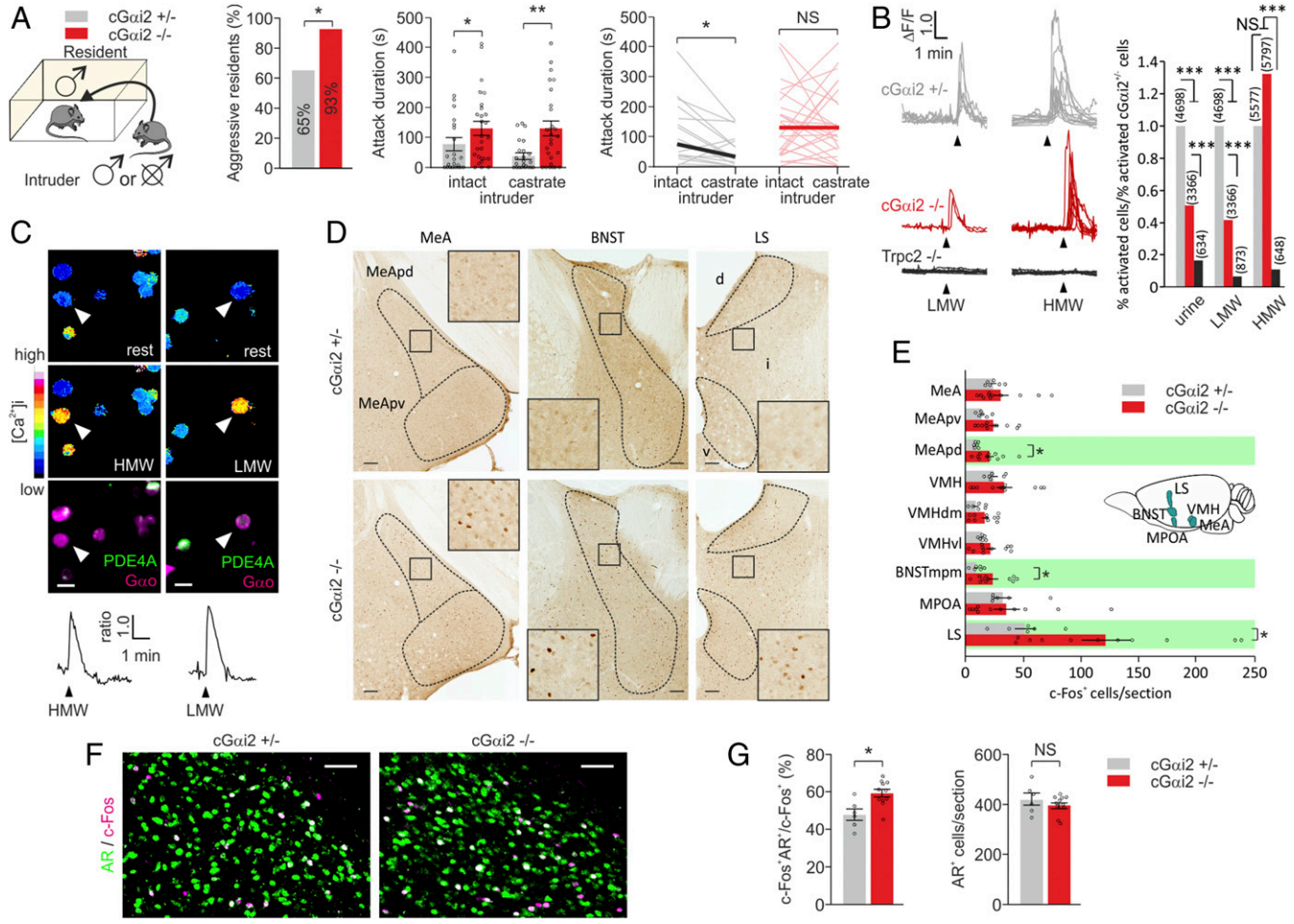

Fig. 3. Loss of Gαi2 enhances territorial aggression and increases activity in aggression-controlling brain centers. (*A*) Territorial aggression is enhanced in sexually experienced cGαi2$^{-/-}$ resident males exposed to intact and castrated intruders in the resident–intruder assay. Fifteen of 23 cGαi2$^{+/-}$ mice (65%) and 25 of 27 (93%) cGαi2$^{-/-}$ resident males were aggressive at least once during three consecutive resident–intruder trials to intact and castrated male intruders (*$P < 0.05$, Fisher's exact test). Cumulative attack duration was higher in cGαi2$^{-/-}$ residents (**$P < 0.01$ and *$P < 0.05$, Mann–Whitney *U* test). Comparison of cGαi2$^{+/-}$ residents' behavior toward gonadally intact vs. castrated intruders indicates the normal reduction in aggression toward a castrate (*$P < 0.05$, Wilcoxon test). This behavior is lost in the cGαi2$^{-/-}$ residents [nonsignificant (NS), $P = 0.8$, Wilcoxon test]. (*B*) Examples of Ca^{2+} transients (*Left*) imaged in dissociated VSNs of cGαi2$^{+/-}$, cGαi2$^{-/-}$, and Trpc2$^{-/-}$ mice stimulated with LMW (1:100) and HMW (1:100) fractions. Analysis of responding cells over total cGαi2$^{+/-}$ responding cells (*Right*) reveals reduced responsivity to urine (1:100) and LMW fraction in cGαi2$^{-/-}$ cells and a loss in Trpc2$^{-/-}$ cells (***$P < 0.001$; NS, $P = 0.2$, Fisher's exact test). Number of cells analyzed is indicated above each bar. Each stimulus was tested in 3–20 mice. (*C*) Fura-2 ratio imaging and post hoc IHC of cGαi2$^{-/-}$ cells indicate that cells activated by LMW and HMW fractions are Gαo^{+} and PDE4A^{-}. Time points of Ca^{2+} images show resting or peak fluorescence levels to stimulation with HMW or LMW fractions. Representative Ca^{2+} transients shown for imaged cells (white arrowheads) are indicated for each condition. (Scale bar, 10 μm.) (*D*) Examples of c-Fos activation in MeA, BNST, and LS of cGαi2$^{+/-}$ and cGαi2$^{-/-}$ male mice exposed to intact male intruder for 10 min. Dashed lines indicate the border of brain areas. Boxes are shown at higher magnification in the *Inset*. (Scale bars, 100 μm.) (*E*) Quantification of c-Fos^{+} cells per section in cGαi2$^{+/-}$ ($n = 6$) and cGαi2$^{-/-}$ residents ($n = 11$) after exposure to an intact intruder reveals an increase in c-Fos expression in MeApd, BNSTmpm, and LS of cGαi2$^{-/-}$ mice (marked in green; *$P < 0.05$; NS, $P = 0.15$–0.99, Mann–Whitney *U* test). (*F*) Gαi2 deletion resulted in increased c-Fos activation of a population of GABAergic, AR^{+} neurons in the MeApd following a 10-min exposure to an intact male intruder. (*G*) Percentage of c-Fos^{+} neurons expressing AR (*Left*) and number of AR^{+} cells per section (*Right*) in the MeApd after a 10-min exposure to an intact male intruder (*$P < 0.05$; NS, $P = 0.46$, Mann–Whitney *U* test). (Scale bars, 50 μm.) d, dorsal LS; i, intermediate LS; v, ventral LS. Data are expressed as means ± SEM.

4 *C* and *D*). We compared the density of c-Fos^{+} nuclei of cGαi2$^{-/-}$ males vs. cGαi2$^{+/-}$ males following pup exposure. In the granular layer of the anterior AOB, c-Fos^{+} cell density was significantly lower in parental cGαi2$^{-/-}$ males vs. aggressive cGαi2$^{+/-}$ male mice ($P < 0.001$; Fig. 4 *C* and *D*), consistent with reduced sensory input from the apical VNO in these mutants. Aggressive cGαi2$^{+/-}$ males also showed more c-Fos^{+} cells in the MeApv and MeApd compared with cGαi2$^{-/-}$ males, suggesting that Gαi2-dependent sensory inputs elicit MeA activation and infant-directed aggression. We also investigated the MPOA of the hypothalamus, a key region in the control of parenting behaviors (45). We observed specific activation during pup interactions in cGαi2$^{-/-}$ males, but this activation was absent in aggressive cGαi2$^{+/-}$ controls (Fig. 4 *C* and *D*). Importantly, our c-Fos mapping revealed significantly higher activation in the medial preoptic nucleus (MPO), the central region of MPOA, of cGαi2$^{-/-}$ males compared with parental controls ($P < 0.05$; Fig. 4 *C* and *D*). Thus, Gαi2-dependent VNO inputs seem to inhibit MPOA activation and subsequent parental behavior.

To identify the activated neurons in the MeA during pup-directed aggression and determine whether they belong to the same AR^{+}, GABAergic neurons activated during male–male aggression, we performed double-label IHC for c-Fos and AR. There was little overlap between c-Fos^{+} and AR^{+} nuclei in aggressive cGαi2$^{+/-}$ males (Fig. 4*E*). c-Fos^{+} nuclei also did not colocalize with CB^{+} or CR^{+} cells in the MeA (*SI Appendix*, Fig. S5).

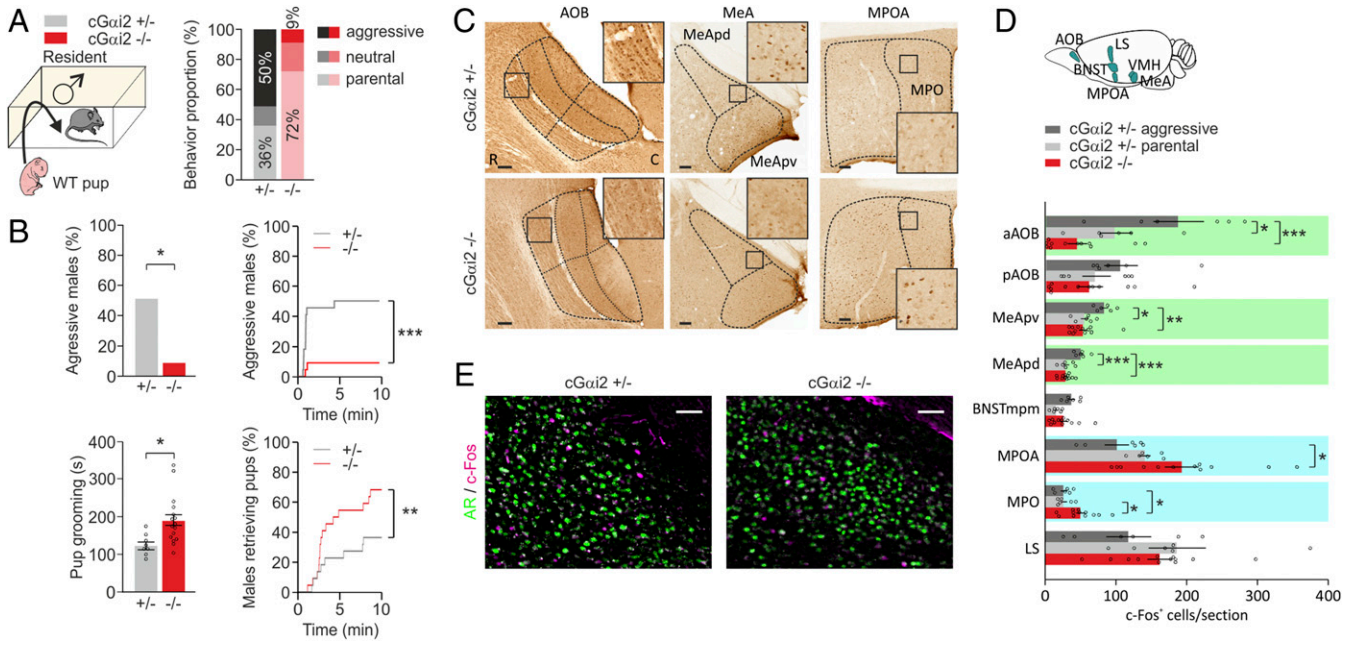

Fig. 4. cGαi2$^{-/-}$ male mice show diminished infant-directed aggression but enhanced parental behavior. (*A*) Comparison of pup-directed behavior of adult cGαi2$^{+/-}$ vs. cGαi2$^{-/-}$ male residents. Pups (WT) were used at postnatal days 1–2. Males attacked (aggressive), ignored (neutral), or retrieved neonates to the nest (parental behavior). cGαi2$^{-/-}$ males were predominantly parental (72%), whereas cGαi2$^{+/-}$ males attacked the pups (50%; $n = 22$ for each genotype). (*B*) Percentages of aggressive males (*$P < 0.05$, Fisher's exact test) and their latency to attack the neonates (***$P < 0.001$, Kolmogorov–Smirnov test), pup grooming times of the cGαi2$^{+/-}$ ($n = 8$) and cGαi2$^{-/-}$ residents ($n = 16$) that showed the behavior [*t* test: $t(22) = 2.73$, *$P < 0.05$], and percentage of males retrieving pups (**$P < 0.01$, Kolmogorov–Smirnov test). (*C*) Examples of c-Fos activation in AOB, MeA, and MPOA of cGαi2$^{+/-}$ and cGai2$^{-/-}$ males exposed to an alien pup for 10 min. Dashed lines indicate brain areas where c-Fos^{+} cells were counted. Boxes are shown at higher magnification in the *Inset*. C, caudal; R, rostral. (Scale bars, 100 μm.) (*D*) Quantification of c-Fos^{+} cells per section of aggressive cGαi2$^{+/-}$ ($n = 6$), parental cGαi2$^{+/-}$ ($n = 6$), and cGαi2$^{-/-}$ residents ($n = 12$) after exposure to an alien pup reveals increased c-Fos activation in aAOB, MeApd, and MeApv of aggressive cGαi2$^{+/-}$ males [aAOB, $F(2,21) = 10.72$, $P < 0.001$; MeApd, $F(2,21) = 13.98$, $P < 0.001$; MeApv, $F(2,21) = 6.075$, $P < 0.001$, ANOVA; *$P < 0.05$, **$P < 0.01$, ***$P < 0.001$, Tukey test; green]. Enhanced activation is observed in the MPOA (MPO) of cGαi2$^{-/-}$ males [MPOA, $F(2,21) = 5.236$, $P < 0.05$; MPO, $F(2,21) = 4.377$, $P < 0.05$, ANOVA; *$P < 0.05$, Tukey test; blue]. No significant differences are observed in other regions analyzed ($P = 0.06$–0.81, ANOVA). (*E*) Conditional Gαi2 deletion does not cause c-Fos activation of a population of GABAergic, AR^{+} neurons in the MeApd following a 10-min exposure to neonates. (Scale bar, 50 μm.) aAOB, anterior AOB; pAOB, posterior AOB. Data are expressed as means ± SEM.

Therefore, the MeA neurons activated during pup-directed aggression are distinct from those activated during male–male aggression. Together, these results provide strong support for a model in which Gαi2^{+} VSNs control infant-directed aggression by activation of specific aggression nodes that, in turn, inhibit parental-specific circuits.

Discussion

Our results show that the Gαi2^{+} population of VSNs controls important aspects of male–male and infant-directed aggression. We identify Gαi2 as the primary G protein α-subunit mediating the detection of small organic chemosignals by apical VSNs, most likely being responsible for activation of Trpc2 and subsequent Ca^{2+} entry downstream of V1R activation. Gαi2 is an abundant G protein expressed in major cognitive centers such as the cortex and is important for its development, and complete loss or reduction of Gαi2 signaling can result in defective social interaction, increased anxiety, and intellectual disability (27). Therefore, a global Gαi2 mutation may impede investigations of complex VNO-dependent social behaviors. Indeed, our results differ from a report that used global Gαi2-KO mice that exhibited reduced male–male aggression (23). The conditional, olfactory-restricted KO model developed here ablated Gαi2 only in *Omp*-expressing cells, indicating that the observed behavioral deficits depend on the olfactory system. *Omp* is highly expressed in mature sensory neurons of MOE and VNO (46). Although Gαi2 is also expressed in some sensory neurons of the MOE (47), Gαi2 does not seem to participate in known sensory signaling events (48). Our conditional KO mice showed no obvious defects in MOE or MOB morphology and odor-guided behaviors depending on a functional MOE, indicating that the behavioral phenotypes we observe are largely mediated by VNO function.

We found that conditional deletion of Gαi2 suppresses infanticidal behavior, consistent with a direct role of Gαi2 in the detection of pup odor. Furthermore, c-Fos mapping showed less activation in downstream brain areas of the Gαi2 vomeronasal pathway—aAOB and MeA—in Gαi2-deficient virgin male mice exposed to pups. Interestingly, Gαi2 mutant male mice became parental after contact with pups and showed elevated c-Fos in the MPOA, suggesting that this circuit may inhibit proparental MPOA neurons (49). Thus, infanticidal behavior seems to involve the activation of a dedicated circuit, rather than being merely a consequence of the inhibition of parenting behavior.

Our Gαi2 mutant males displayed high levels of male–male aggression, indicating that the Gαi2 subpopulation of VSNs is dispensable for triggering this behavior. Therefore, male–male and infant-directed aggression are initiated by different subsets of VSNs, suggesting that distinct accessory olfactory system circuits control the display of these two forms of aggression. Consistent with this, c-Fos analysis revealed the activation of different populations of MeA neurons in the context of each behavior. Many of these cells were positive for AR in the male–male aggression assay but negative for AR in the pup-directed aggression test. Because deletion of Gαo in the VNO eliminated male–male aggression (16), Gαo^{+} VSNs are probably the key drivers of aggression induced by LMW and HMW urine fractions. The LMW fraction, which includes peptides <10 kDa, is still partially

detected by VSNs from Gαi2-deficient mice, suggesting that LMW-induced aggression is controlled via detection of $G\alpha o^+$ VSNs. However, the $G\alpha o^+$ VSN population is unlikely to govern male–male aggression independently. Gαi2-deficient mice tended to be more aggressive to intact and castrated males, suggesting that $G\alpha i2^+$ VSNs can influence male–male aggression, perhaps by eliciting partial inhibition on Gαo- and/or MOE-dependent targets in limbic brain areas. Consistent with this, we observed higher c-Fos activation in the MeA, BNST, and LS of Gαi2-deficient mice when exposed to males. Similar roles for VNO signaling in inhibiting social behaviors have been observed for sexual behavior toward young conspecifics (50). Thus, $G\alpha o^+$ and $G\alpha i2^+$ VSN populations seem to interact reciprocally to modulate male–male aggression.

Interestingly, we found no difference between Gαi2-deficient males and their heterozygous controls in mounting behavior, indicating that $G\alpha i2^+$ VSNs are not required for mating motivation in males. These results, together with studies in Trpc2 and Gαo mutants (16, 41, 42), are consistent with a relatively minor role of the VNO in the display of male mating behavior. In *Trpc2* mutant mice, however, sex preference is strongly affected, as mutant males attempt to mate with males as frequently as with females (41, 42). By contrast, Gαi2 and Gαo mutant males showed a clear preference for females (ref. 16 and the present study), suggesting that both VNO layers interact to enable sex preference.

Taken together, our results suggest a role of Gαi2 as key element in the coupling of activated V1R receptors to the downstream signal transduction machinery. Downstream signaling has been proposed to occur via Gγ13 because of coexpression with Gαi2 (51). However, because of the absence of functional measurements at the cellular level and the complexity of behavioral phenotype interpretation of Gγ13-null mice—probably affected by a critical function of Gγ13 in MOE signaling and olfaction (52)—this role has not been confirmed thus far. It has been proposed that Gαi2 may also interact with formyl peptide receptors and canonical olfactory receptors, which are mostly expressed in the apical layer of the VNO (53–55). Notably, VSNs expressing *Olfr692* seem to be activated by odors emanating from pups, especially in virgin males, suggesting a potential *Olfr692* role in infant-directed aggression (56). However, *Olfr692* is expressed in basal $G\alpha o^+$ VSNs (56), and no direct functional link has been yet established between *Olfr692* and infanticide. A recent report linked infant-derived chemosensory activity with seven vomeronasal receptors, including three V1Rs and four V2Rs, two of which (Vmn2r65 and Vmn2r88) seem to be partially implicated in infanticide (57). Together with our findings, these results support a non–labeled-line model for infant-directed aggression in which information sensed by apical and basal VSN populations is integrated to generate an aggressive response.

In conclusion, we showed here an essential role of Gαi2 in VNO sensory signaling of the apical VSN population that detects small organic molecules including volatile pheromones and steroid derivatives. Our study identifies $G\alpha i2^+$ VSNs as a critical neural component that organizes and balances male–male and infant-directed aggression. These results provide a framework for dissecting the neuronal networks underlying different forms of social aggression.

Methods

Animal care and experimental procedures were performed in accordance with French, German, and European guidelines on the protection of animals used for scientific purposes and approved by an ethical committee for animal experimentation (Comité d'Etique en Expérimentation Animale Val de Loire and Animal Welfare Committee of Saarland University School of Medicine). Mice were kept under standard 12-h light/dark cycles with food and water ad libitum.

Generation of Conditional Gαi2-Deficient Mice. $Gnai2^{fx/fx}$ mice (mixed 129sv × C57BL/6 background) were crossed to mice carrying a transgene directing the expression of Cre recombinase under the control of the *Omp* promoter [*Omp*-Cre mice; B6; 129P2-$Omp^{tm4(cre)Mom}$/MomJ; Jackson Laboratory, JR 006668; backcrossed into C57BL6/J for eight generations; neomycin cassette absent]. $Gnai2^{fx/fx}$ mice carry *loxP* sites inserted into the introns that flank exons 2 and 4. Breeding established offspring ($cG\alpha i2^{-/-}$) that were homozygous for the floxed *Gnai2* alleles and heterozygous for Cre and *Omp* ($Gnai2^{fx/fx}$ $Omp^{cre/+}$). In these mice, Cre-mediated *Gnai2* deletion was restricted to *Omp*-positive cells. Animals heterozygous for both alleles ($Gnai2^{fx/+}$ $Omp^{cre/+}$) served as controls ($cG\alpha i2^{+/-}$). Homozygous mice containing the Rosa-CAG-LSL-GCaMP6f::ΔNeo conditional allele [B6;129S-*Gt (ROSA)26Sor*$^{tm95.1(CAG-GCaMP6f)Hze}$/J; Jackson Laboratory] were crossed with $Gnai2^{fx/fx}$ to produce mice homozygous for Rosa-CAG-LSL-GCaMP6f::ΔNeo and floxed *Gnai2* alleles. These mice were crossed with homozygous $Gnai2^{fx/fx}$ $Omp^{cre/cre}$ mice to yield mice homozygous for the floxed *Gnai2* allele and heterozygous for Cre, *Omp*, and GCaMP6f ($cG\alpha i2^{-/-}$ $GCaMP6f^{+/-}$). Animals heterozygous for all alleles ($Gnai2^{fx/+}$ $Omp^{cre/+}$ $GCaMP6f^{fx/+}$) served as controls ($cG\alpha i2^{+/-}$ $GCaMP6f^{+/-}$). $Trpc2^{-/-}$ (129S6.129P2-*Trpc2* < *tm1Mom*>/MomJ; Jackson Laboratory, JR 007890; backcrossed into C57BL/6J for six generations) (58) were used for Ca^{2+} imaging in dissociated VSNs. Adults males (8–12 wk) were used.

Immunostaining. Mice were anesthetized by an overdose of pentobarbital (Ceva) and perfused transcardially with 0.9% saline solution followed by 0.1 M phosphate buffer (PB) containing 4% paraformaldehyde (PFA). For c-Fos experiments, mice were perfused 90 min after a 10-min interaction with an intact male or a neonate. Brains, VNOs, and MOEs were removed, post-fixed overnight in 4% PFA, and cryoprotected in 0.1 M PB containing 30% sucrose. Samples were embedded in Tissue-Tek O.C.T. compound, snap-frozen in cold isopentane, and processed on a Leica CM 3050S cryostat. Brains and OBs were cut in 30-μm serial free-floating sections (coronal for brains, sagittal for OB) by using Tris-buffered saline (TBS) solution containing 0.1% sodium azide. Coronal cryosections of olfactory tissues (12-μm thick) were directly mounted on SuperFrost Plus glass slides. Sections were washed (3 × 5 min) with TBS, incubated in blocking solution (TBS solution containing 0.1% Triton X-100 and 5% horse serum) for 2 h at room temperature (RT), incubated overnight at 4 °C in blocking solution supplemented with the primary antibody, and washed in TBS solution and incubated in blocking solution supplemented with secondary antibody for 2 h at RT. Nuclei were counterstained with DAPI (0.5 μg/mL; Sigma) for 5 min. For c-Fos experiments, endogenous peroxidases were blocked for 30 min in TBS solution containing 3% H_2O_2 before the serum blocking step, biotinylated secondary antibody was used, and signals were amplified with Vectastain ABC kit (Vector) and visualized with diaminobenzidine (0.02%, 0.01% H_2O_2 in 0.05 M Tris, pH 7.4). Detailed information about the antibodies used is listed in *SI Appendix*, Table S1. VNO cell density, VNO layer, and AOB volume quantifications were done from images acquired on an Olympus IX71 microscope coupled to a Hamamatsu C10600-10B camera at 10× magnification. Images were analyzed with Fiji/ImageJ [National Institutes of Health (NIH)]. Twenty-five slices of VNO from adult males (five of each genotype) were used. Demarcations of apical vs. basal layers were based on PDE4A immunoreactivity, and $DAPI^+$ cells were counted by using the particle analyzer plugin of Fiji. AOB rostrocaudal demarcation was based on Gαo immunoreactivity from 29 slices from 14 animals per genotype. Tissue volume in cubic micrometers was calculated by multiplying the surface of the immunoreactive area by the thickness of the slice. For c-Fos experiments, slices were scanned by using an automatic slide scanner (AxioScan.Z1; Zeiss). Regions of interest (ROIs) were drawn based on the Paxinos mouse brain atlas by using Zen (blue edition 3.0; Zeiss), and the number of $c\text{-}Fos^+$ cells was automatically counted bilaterally in these regions by using the particle analyzer plugin of Fiji. Numbers of slices counted per animal and region were one for the MPOA and LS; two for AOB, BNST, and VMH; and four for MeA. AR/c-Fos coexpression was quantified in five to eight MeApd images per animal acquired on a Zeiss LSM-700 confocal laser-scanning microscope at 20× magnification. Image regions were analyzed in the entire *z* axis with 3-μm step intervals, and images were reconstituted by using the maximum-intensity projection tool of Zen software. $c\text{-}Fos^+$, AR^+, and $AR/c\text{-}Fos^+$ cells were counted automatically by using the particle analyzer plugin of Fiji.

For combined Ca^{2+} imaging and immunocytochemistry, dissociated VNO cells were fixed by using PBS solution containing 4% PFA (10 min), permeabilized and incubated for 10 min in blocking solution (TST, i.e., 0.1% Triton X-100, 1% FBS, 50 mM NaCl, 100 mM Tris·HCl, pH 7.5), incubated with anti-PDE4A (1:500; 30 min, RT) and anti-Gαo (1:50; 30 min, RT), and washed in TST (5 min), followed by an incubation (30 min, RT) in secondary

NEUROSCIENCE

antibodies (Alexa Fluor 488 goat anti-rabbit, Alexa Fluor 647 goat anti-mouse, 1:500; Invitrogen). Cells were also stained (5 min, RT) with DAPI.

Quantitative RT-PCR. VNOs and MOEs were dissected from cGαi2$^{+/-}$ and cGαi2$^{-/-}$ mice. Pools of VNO or MOE from three animals were established from a total of 21 VNOs and 9 MOEs per genotype. RNA in each pool was isolated with PureLink RNA Mini Kit (Invitrogen). cDNA was synthesized from 1 μg of total RNA by using a Superscript III First-Strand Synthesis System for RT-PCR (Invitrogen). Quantitative PCRs were performed on a CFX96 Touch Real-Time PCR Detection System (Bio-Rad) using SsoAdvanced Universal SYBR green Supermix (Bio-Rad). PCR conditions for all primers were 95 °C for 3 min followed by 39 cycles (95 °C for 10 s, 60 °C for 30 s). PCR specificity was verified by melting curve analysis. Expression of *Hprt-1*, *Omp*, *Gnai2*, and *Gnao* mRNAs were assessed. Each sample was run in triplicate, and data were analyzed with the CFX Manager 3.0 Software (Bio-Rad) normalized to *Hprt-1* expression level to obtain a ΔCt and expressed as $2^{\Delta Ct}$. VNO cDNAs were used to assess *V1re6*, *V1re2*, *V1rf3*, *V1rj2*, *Vmn2r1*, *Vmn2r65*, *Trpc2*, and *Plcb2* expression by endpoint PCR with GoTaq G2 Master Mix. Primer sequences are shown in *SI Appendix*, Table S2. PCR conditions for all primers were 95 °C for 3 min, followed by 39 cycles (95 °C for 45 s, 58 °C for 30 s, and 72 °C for 60 s), and 72 °C for 10 min. Products were run on a 1% agarose gel.

Ca^{2+} Imaging. Ca^{2+} imaging of freshly dissociated VSNs was performed as described previously (15, 16). VNO epithelium was detached from the cartilage and minced in PBS solution at 4 °C. The tissue was incubated (20 min at 37 °C) in PBS solution supplemented with papain (0.22 U/mL) and DNase I (10 U/mL; Fermentas), gently extruded in DMEM (Invitrogen) supplemented with 10% FBS, and centrifuged at 100 × *g* (5 min). Dissociated cells were plated on coverslips previously coated with concanavalin-A type V (0.5 mg/mL, overnight at 4 °C; Sigma). Cells were used immediately for imaging after loading them with fluo-4/AM or fura-2/AM (5 μM; Invitrogen) for 60 min. Coverslips containing VSNs were placed in a laminar-flow chamber (Warner Instruments) and constantly perfused at 22 °C with extracellular solution HBSS (Invitrogen) supplemented with 10 mM Hepes (2-[4-(2-hydroxyethyl) piperazin-1-yl]ethanesulfonic acid). Cells were alternately illuminated at 470 nm for fluo-4 or at 340 and 380 nm for fura-2 imaging, and light emitted above 510 nm was recorded by using a Hamamatsu C10600-10B camera installed on an Olympus IX71 microscope. Images were acquired at 0.25 Hz and analyzed by using ImageJ (NIH), including background subtraction, ROI detection, and signal analyses. ROIs were selected manually and always included the whole cell body. Peak signals were calculated from the temporal profiles of image ratio/fluorescent values. Results are based on recordings from at least three mice for each condition and genotype.

VNO tissue slices were prepared from male cGαi2$^{+/-}$ GCaMP6f$^{+/-}$ and cGαi2$^{-/-}$ GCaMP6f$^{+/-}$ mice by using slicing procedures established previously (33, 34, 39). Briefly, mice were euthanized with CO_2, followed by decapitation. VNOs were quickly removed and submerged in oxygenated extracellular solution 1 (95% O_2/5% CO_2) containing (in mM): 120 NaCl, 25 $NaHCO_3$, 5 KCl, 5 BES, 1 $MgSO_4$, 1 $CaCl_2$, and 10 mM glucose (300 mOsm). The vomer bones were removed, the VNO was embedded in 3% low-gelling temperature agarose, and coronal slices (250 μm) were cut on a vibratome (Microm HM 650 V). VNO tissues slices were imaged by using an upright scanning confocal microscope (LSM 880 Indimo; Zeiss) equipped with a 20 × 1.0 N.A. Plan-Apochromat water-immersion objective and a standard Argon laser for excitation at a wavelength of 488 nm (GCaMP6f excitation). Emitted fluorescence was collected between 500 and 550 nm. All scanning head settings were kept constant during each experiment. Optical sections were ∼7 μm thick. All scanning head settings (i.e., gain, black level, detector aperture, and laser neutral density filter) were kept constant during each experiment. GCaMP6 fluorescence changes are expressed as relative fluorescence changes, i.e., ΔF/F0 (F0 was the average of the fluorescence values 10 s before stimulation). Images were acquired at 1 Hz and analyzed by using a combination of Zen (Zeiss), ImageJ (NIH), and Igor (Wavemetrics) software. To identify and mark responding VSNs, ΔF images (F−F0) were overlaid onto transmitted light images (Fig. 2*C*) by using Adobe Photoshop's difference tool and slightly adjusting the exposure settings. Original ΔF images of ligand-induced VSN responses are shown in *SI Appendix*, Fig. S2*D*. VNO slices were stimulated successively and in random order by using bath application. The following criteria for stimulus-induced Ca^{2+} responses were applied. (*i*) A response was defined as a stimulus-dependent deviation of GCaMP6f fluorescence that exceeded twice the SD of the mean of the baseline fluorescence noise. (*ii*) Cells showing a response to control buffer were excluded from analysis. (*iii*) A response had to occur within 1 min after stimulus application. In time-series experiments, ligand application was repeated to confirm the repeatability of a given Ca^{2+} response.

Chemostimulation. Chemostimuli for Ca^{2+} imaging were freshly prepared each day and diluted in extracellular solution to give the following final concentrations: urine and HMW and LMW fractions, 1:100 dilution; 2-heptanone, 10^{-8} M (Sigma); 2,5-dimethylpyrazine, 10^{-6} M (Sigma); isobutylamine, 10^{-7} M (Sigma); isoamylamine, 10^{-7} M (Sigma); β-estradiol, 1 μM (E2, Sigma); 1,3,5 (10)-estratrien-3,17β-diol disulfate, 1 μM (E1050; Steraloid or Sigma); 1,3,5 (10)-estratrien-3,17β-diol 3-sulfate, 1 μM (E1100; Steraloid or Sigma); 1,3,5(10)-estratrien-3,17α-diol 3-sulfate, 1 μM (E0893; Steraloid); A7864, 1 μM (5-androsten-3β,17β-diol disulfate; Steraloid); sulfated estrogen mix (E mix) E1050, E1100, E0893, and A7864, each 1 μM; MHC peptide mix SYFPEITHI, SYIPSAEKI, AAPDNRETF, SIINFEKL, 10^{-10} M each (Genscript); and KCl, 50 mM or 60 mM (slice experiments). Sulfated estrogens were initially prepared in DMSO and further diluted in extracellular solution. C57BL/6 males (8–12 wk old; Janvier) served as urine donors. Animals were sexually naïve and were kept group-housed. Equal volumes of freshly collected urine from at least three animals were pooled. To obtain urine fractions, 0.5 mL of fresh urine was size-fractionated by centrifugation (14,000 × *g* for 30 min) by using Microcon (Millipore) or Nanosep (Pall) 10-kDa molecular mass cutoff ultrafiltration columns. The centrifugation supernatant was the LMW fraction, and, to obtain HMW fraction, the retentate was washed with 0.5 mL PBS solution three times and resuspended in 0.5 mL of PBS or oxygenated extracellular solution.

Behavioral Testing. Males were individually housed for 1 wk before testing. Mice were moved to the experimental room 2 h before testing. Assays were conducted 2 h before the start of the dark period.

Resident–intruder male–male aggression assay. Sexually experienced male mice of each genotype (23 cGαi2$^{+/-}$ and 27 cGαi2$^{-/-}$) were tested for territorial aggression. Testing lasted 10 min and began when a sexually inexperienced, gonadally intact, group-housed adult male (i.e., intruder) was placed into the home cage of the test mouse (i.e., resident), whose bedding had not been changed for at least 4 d. Each resident was exposed three times (on consecutive days) to a gonadally intact intruder. After 1 wk, the experiments were repeated with a castrated intruder. Juvenile (postnatal day 18–22) males were castrated under isoflurane general anesthesia and used in adulthood. Residents were not exposed twice to the same intruder. Aggressive behavior was defined as lunging, biting, chasing, tail rattling, wrestling, and kicking. Attack bouts were defined as a succession of aggressive events separated by <3 s. Cumulative attack duration of three consecutive tests, investigation time of the intruder, and number of mounting episodes were scored.

Pup-directed behaviors. Twenty-two sexually naïve males of each genotype were tested for behavior in the presence of an alien 1–2-d-old neonate (C57BL/6 WT) introduced into the home cage of the test mouse for 10 min. To minimize handling and stress to the pups, one single pup was taken from the nest immediately before the test, avoiding prolonged exposure to cold. If harmed, the pup was immediately removed and killed to minimize suffering and to avoid cannibalizing without previous killing. Mice were categorized as aggressive if they presented aggressive behavior (e.g., biting, killing) toward a pup, as parental if they retrieved a pup into their nest, and as neutral if they were indifferent to a pup. Latencies to attack a pup and pup grooming time were scored.

Statistics. Statistical analyses were performed by using GraphPad Prism 7.0 (GraphPad Software), OriginPro 2016G, and OriginPro 2017G (OriginLab). Assumptions of normality and homogeneity of variance were tested before conducting the following statistical approaches. Student's *t* test was used to measure the significance of the differences between two distributions. In case the results failed the test of normality, a Mann–Whitney *U* test was performed. For paired data comparisons, we used the Wilcoxon signed-ranks test, and, for categorical data, we used the Fisher's exact test. Multiple groups were compared by using a one-way or two-way ANOVA with Tukey's multiple comparison test as a post hoc comparison or Kruskal–Wallis ANOVA for nonnormal distributions. The probability of error level (i.e., α) was chosen to be 0.05. Unless otherwise stated, results are presented as means ± SEM and documentation of individual data points.

Further details on testosterone measurements, stimulus delivery, and other behavioral tests are provided in *SI Appendix*, *Materials and Methods*. The datasets generated and/or analyzed during the present study are available from the Data Inra Dataverse portal (https://data.inra.fr/).

ACKNOWLEDGMENTS. We thank Roberto Tirindelli for V2R2 antibody; Michael Konzmann, Kevin Poissenot, and Chantal Porte for technical assistance; Kerstin Becker, Lisa-Marie Knieriemen, Deborah Crespin, and Aurelie Gasnier for mouse

husbandry; Marie-Claire Blache for help with imaging experiments; and Anne-Lyse Lainé for help with hormone assays. This work was supported by Deutsche Forschungsgemeinschaft Grants Sonderforschungsbereich 894 Project A17 (to F.Z. and T.L.-Z.) and INST 256/427-1 FUGB (to T.L.-Z.), Institut National de la Recherche Agronomique (INRA) "Physiologie Animale et Systèmes d'Elevage" department (P.C.); National Institutes of Health Intramural Research Program Project Z01-ES-101643 (to L.B.); and a grant from the University of Tours and Region Centre Val de Loire (to A.-C.T.).

1. Scott JP (1966) Agonistic behavior of mice and rats: A review. *Am Zool* 6:683–701.
2. Hrdy SB (1979) Infanticide among animals: A review, classification, and examination of the implications for the reproductive strategies of females. *Ethol Sociobiol* 1:13–40.
3. McCarthy MM, Vom Saal FS (1986) Inhibition of infanticide after mating by wild male house mice. *Physiol Behav* 36:203–209.
4. Chamero P, Leinders-Zufall T, Zufall F (2012) From genes to social communication: Molecular sensing by the vomeronasal organ. *Trends Neurosci* 35:597–606.
5. Liberles SD (2014) Mammalian pheromones. *Annu Rev Physiol* 76:151–175.
6. Brennan PA, Keverne EB (2004) Something in the air? New insights into mammalian pheromones. *Curr Biol* 14:R81–R89.
7. Mohrhardt J, Nagel M, Fleck D, Ben-Shaul Y, Spehr M (2018) Signal detection and coding in the accessory olfactory system. *Chem Senses* 43:667–695.
8. Shinohara H, Asano T, Kato K (1992) Differential localization of G-proteins Gi and Go in the accessory olfactory bulb of the rat. *J Neurosci* 12:1275–1279.
9. Jia C, Halpern M (1996) Subclasses of vomeronasal receptor neurons: Differential expression of G proteins (Gi alpha 2 and G(o alpha)) and segregated projections to the accessory olfactory bulb. *Brain Res* 719:117–128.
10. Berghard A, Buck LB (1996) Sensory transduction in vomeronasal neurons: Evidence for G alpha o, G alpha i2, and adenylyl cyclase II as major components of a pheromone signaling cascade. *J Neurosci* 16:909–918.
11. Dulac C, Axel R (1995) A novel family of genes encoding putative pheromone receptors in mammals. *Cell* 83:195–206.
12. Matsunami H, Buck LB (1997) A multigene family encoding a diverse array of putative pheromone receptors in mammals. *Cell* 90:775–784.
13. Ryba NJ, Tirindelli R (1997) A new multigene family of putative pheromone receptors. *Neuron* 19:371–379.
14. Herrada G, Dulac C (1997) A novel family of putative pheromone receptors in mammals with a topographically organized and sexually dimorphic distribution. *Cell* 90:763–773.
15. Chamero P, et al. (2007) Identification of protein pheromones that promote aggressive behaviour. *Nature* 450:899–902.
16. Chamero P, et al. (2011) G protein G(alpha)o is essential for vomeronasal function and aggressive behavior in mice. *Proc Natl Acad Sci USA* 108:12898–12903.
17. Hattori T, et al. (2016) Self-exposure to the male pheromone ESP1 enhances male aggressiveness in mice. *Curr Biol* 26:1229–1234.
18. Kaur AW, et al. (2014) Murine pheromone proteins constitute a context-dependent combinatorial code governing multiple social behaviors. *Cell* 157:676–688.
19. Leinders-Zufall T, et al. (2014) A family of nonclassical class I MHC genes contributes to ultrasensitive chemodetection by mouse vomeronasal sensory neurons. *J Neurosci* 34: 5121–5133.
20. Oboti L, et al. (2014) A wide range of pheromone-stimulated sexual and reproductive behaviors in female mice depend on G protein Gαo. *BMC Biol* 12:31.
21. Pérez-Gómez A, et al. (2015) Innate predator odor aversion driven by parallel olfactory subsystems that converge in the ventromedial hypothalamus. *Curr Biol* 25: 1340–1346.
22. Novotny M, Harvey S, Jemiolo B, Alberts J (1985) Synthetic pheromones that promote inter-male aggression in mice. *Proc Natl Acad Sci USA* 82:2059–2061.
23. Norlin EM, Gussing F, Berghard A (2003) Vomeronasal phenotype and behavioral alterations in G alpha i2 mutant mice. *Curr Biol* 13:1214–1219.
24. Wu Z, Autry AE, Bergan JF, Watabe-Uchida M, Dulac CG (2014) Galanin neurons in the medial preoptic area govern parental behaviour. *Nature* 509:325–330.
25. Tachikawa KS, Yoshihara Y, Kuroda KO (2013) Behavioral transition from attack to parenting in male mice: A crucial role of the vomeronasal system. *J Neurosci* 33: 5120–5126.
26. Trainor BC, Sisk CL, Nelson RJ (2009) Hormones and the development and expression of aggressive behavior. *Hormones, Brain and Behavior*, eds Pfaff DW, Arnold AP, Etgen AM, Fahrbach SE, Rubin RT (Academic, San Diego), 2nd Ed, pp 167–205.
27. Hamada N, et al. (2017) Role of a heterotrimeric G-protein, Gi2, in the corticogenesis: Possible involvement in periventricular nodular heterotopia and intellectual disability. *J Neurochem* 140:82–95.
28. Rudolph U, et al. (1995) Ulcerative colitis and adenocarcinoma of the colon in G alpha i2-deficient mice. *Nat Genet* 10:143–150.
29. Ustyugova IV, Zhi L, Abramowitz J, Birnbaumer L, Wu MX (2012) IEX-1 deficiency protects against colonic cancer. *Mol Cancer Res* 10:760–767.
30. Li J, Ishii T, Feinstein P, Mombaerts P (2004) Odorant receptor gene choice is reset by nuclear transfer from mouse olfactory sensory neurons. *Nature* 428:393–399.
31. Weiss J, et al. (2011) Loss-of-function mutations in sodium channel Nav1.7 cause anosmia. *Nature* 472:186–190.
32. Tanaka M, Treloar H, Kalb RG, Greer CA, Strittmatter SM (1999) G(o) protein-dependent survival of primary accessory olfactory neurons. *Proc Natl Acad Sci USA* 96:14106–14111.
33. Leinders-Zufall T, et al. (2004) MHC class I peptides as chemosensory signals in the vomeronasal organ. *Science* 306:1033–1037.
34. Leinders-Zufall T, et al. (2000) Ultrasensitive pheromone detection by mammalian vomeronasal neurons. *Nature* 405:792–796.
35. Isogai Y, et al. (2011) Molecular organization of vomeronasal chemoreception. *Nature* 478:241–245.
36. Haga-Yamanaka S, et al. (2014) Integrated action of pheromone signals in promoting courtship behavior in male mice. *eLife* 3:e03025.
37. Del Punta K, et al. (2002) Deficient pheromone responses in mice lacking a cluster of vomeronasal receptor genes. *Nature* 419:70–74.
38. Leinders-Zufall T, Ishii T, Mombaerts P, Zufall F, Boehm T (2009) Structural requirements for the activation of vomeronasal sensory neurons by MHC peptides. *Nat Neurosci* 12:1551–1558.
39. Sturm T, et al. (2013) Mouse urinary peptides provide a molecular basis for genotype discrimination by nasal sensory neurons. *Nat Commun* 4:1616.
40. Kelliher KR, Spehr M, Li XH, Zufall F, Leinders-Zufall T (2006) Pheromonal recognition memory induced by TRPC2-independent vomeronasal sensing. *Eur J Neurosci* 23: 3385–3390.
41. Leypold BG, et al. (2002) Altered sexual and social behaviors in trp2 mutant mice. *Proc Natl Acad Sci USA* 99:6376–6381.
42. Stowers L, Holy TE, Meister M, Dulac C, Koentges G (2002) Loss of sex discrimination and male-male aggression in mice deficient for TRP2. *Science* 295:1493–1500.
43. Hong W, Kim D-W, Anderson DJ (2014) Antagonistic control of social versus repetitive self-grooming behaviors by separable amygdala neuronal subsets. *Cell* 158:1348–1361.
44. Blake CB, Meredith M (2011) Change in number and activation of androgen receptor-immunoreactive cells in the medial amygdala in response to chemosensory input. *Neuroscience* 190:228–238.
45. Numan M (1974) Medial preoptic area and maternal behavior in the female rat. *J Comp Physiol Psychol* 87:746–759.
46. Margolis FL (1980) A marker protein for the olfactory chemoreceptor neuron. *Proteins of the Nervous System* (Raven Press, New York), pp 59–84.
47. Ibarra-Soria X, Levitin MO, Saraiva LR, Logan DW (2014) The olfactory transcriptomes of mice. *PLoS Genet* 10:e1004593.
48. Scholz P, et al. (2016) Identification of a novel Gnao-mediated alternate olfactory signaling pathway in murine OSNs. *Front Cell Neurosci* 10:63.
49. Kohl J, Autry AE, Dulac C (2017) The neurobiology of parenting: A neural circuit perspective. *BioEssays* 39:1–11.
50. Ferrero DM, et al. (2013) A juvenile mouse pheromone inhibits sexual behaviour through the vomeronasal system. *Nature* 502:368–371.
51. Liu Q, Li S, Lu C, Yu CR, Huang L (2018) G protein γ subunit Gγ13 is essential for olfactory function and aggressive behavior in mice. *Neuroreport* 29:1333–1339.
52. Li F, et al. (2013) Heterotrimeric G protein subunit Gγ13 is critical to olfaction. *J Neurosci* 33:7975–7984.
53. Liberles SD, et al. (2009) Formyl peptide receptors are candidate chemosensory receptors in the vomeronasal organ. *Proc Natl Acad Sci USA* 106:9842–9847.
54. Rivière S, Challet L, Fluegge D, Spehr M, Rodriguez I (2009) Formyl peptide receptor-like proteins are a novel family of vomeronasal chemosensors. *Nature* 459:574–577.
55. Lévai O, Feistel T, Breer H, Strotmann J (2006) Cells in the vomeronasal organ express odorant receptors but project to the accessory olfactory bulb. *J Comp Neurol* 498: 476–490.
56. Nakahara TS, et al. (2016) Detection of pup odors by non-canonical adult vomeronasal neurons expressing an odorant receptor gene is influenced by sex and parenting status. *BMC Biol* 14:12.
57. Isogai Y, et al. (2018) Multisensory logic of infant-directed aggression by males. *Cell* 175:1827–1841.e17.
58. Bleymehl K, et al. (2016) A sensor for low environmental oxygen in the mouse main olfactory epithelium. *Neuron* 92:1196–1203.